

Communications

Low Angle Scattering From 2-D Targets on a Time-Evolving Sea Surface

R. J. Burkholder, M. R. Pino, and F. Obelleiro

Abstract—The results of a numerical investigation of the electromagnetic scattering from two-dimensional (2-D) targets on a time-evolving sea surface are presented. The 2-D radar cross section (RCS), or “echo width,” is computed as a function of time as the sea surface evolves linearly using the spectrally accelerated generalized forward-backward method. It is shown that the RCS varies with time on the order of seconds, which is much longer than the typical pulse width or pulse repetition rate of search radars. It is also observed that for low-grazing angles of incidence the primary sea surface influence on the RCS comes from the long waves in the ocean spectrum.

Index Terms—Integral equations, iterative methods, marine vehicles, remote sensing, rough surfaces, sea surface.

I. INTRODUCTION

The electromagnetic (EM) scattering from a target on a rough sea surface can be significantly affected by the prevailing sea state [1]–[3]. Not only must the target be detected in the presence of a random rough surface, but the surface changes with time as the ocean waves propagate. Most previous studies of this problem have considered the scattering from a target on a single rough surface realization as a function of the aspect angle [1], [2], or have used Monte Carlo methods to compute the coherent and incoherent scattering from the target on a set of randomly generated surfaces with the same statistics [3]. Other studies have considered the scattering from targets over or under a rough surface [4], some of which use a four path model based on the coherent reflection coefficient of the rough surface [5]–[8]. In this communication the EM scattering from a two-dimensional (2-D) target on a randomly generated sea surface is computed as a function of time as the sea surface evolves. Radar detection algorithms often rely on the calculated coherent backscatter from a target, i.e., the scattering averaged over time or over many different surface realizations within the same sea state. However, the sea surface changes relatively slowly with respect to the pulse width and pulse repetition rate of most radars. Therefore, it is important to understand the time-dependence of the scattering from a target on a realistic time-evolving sea surface.

Recent advances in numerical solutions for rough surface problems have allowed very large surfaces to be modeled [1]–[4], [9]–[12], which is necessary to analyze low-grazing angles of incidence. The spectrally accelerated generalized forward-backward (SAGFB) method [2] is used here to efficiently solve the integral equation associated with a perfectly electrically conducting (PEC) 2-D target on a finite-length randomly generated sea surface as shown in Fig. 1. In this method, the spectral acceleration approach devised in [9] is applied to the generalized forward-backward (GFB) method of [1]. The GFB method is based on the forward-backward (FB) approach of [10], or equivalently,

Manuscript received May 2, 2001; revised January 22, 2002. This work was supported by the United States Office of Naval Research under Grant N00014-98-1-0243.

R. J. Burkholder is with the ElectroScience Laboratory, Department of Electrical Engineering, The Ohio State University, Columbus, OH 43212 USA.

M. R. Pino and F. Obelleiro are with the Department of Tecnoloxías das Comunicacións, Universidade de Vigo, Vigo 36200, Spain.

Publisher Item Identifier S 0196-2892(02)05275-0.

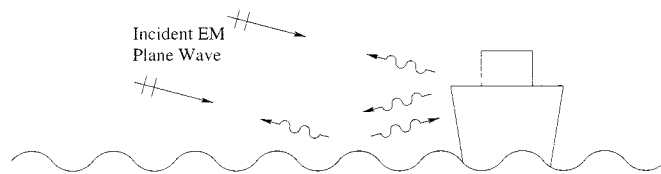


Fig. 1. Geometry of a 2-D ship-like target on a rough sea surface illuminated by an incident plane wave.

the method of ordered multiple interactions [11], but modified to include one or more irregular targets in the presence of an otherwise single-valued quasiplanar surface. For example, the target could be a ship or large breaking wave on a sea surface. The FB and GFB methods have a computational complexity of $\mathcal{O}(N^2)$, where N is the number of unknowns in the discretized integral equation problem. The SAGFB method reduces the computational complexity to $\mathcal{O}(N)$, so surfaces which are very electrically large may be analyzed.

The sea surface is also modeled as a PEC for this study. The frequency used here is 1 GHz and only the horizontal polarization case is considered, so the PEC model of sea water is appropriate as demonstrated in [2]. It is noted that a vertical polarization case is also included in [2] for comparison. A Pierson–Moskowitz ocean wave spectrum is used to generate the random sea surface for a given wind speed, and a linear dispersion relationship is used to propagate the ocean waves [13]–[17]. The numerical model of the surface and target is discussed in more detail in Section II. The backscattering of an incident EM plane wave from some 2-D target shapes in the presence of the sea surface is computed as a function of time for several cases with differing surface roughness and elevation angle of the incident plane wave. The results are presented in Section III. It is seen that the effect of the rough sea surface on the backscatter becomes less significant for lower elevation angles. It is also seen that for low-grazing angles of incidence the primary variations in the backscatter correlate to the propagation of the long ocean waves. Conclusions are discussed in Section IV.

II. DESCRIPTION OF THE NUMERICAL MODEL

The Pierson–Moskowitz infinite-depth ocean model is used to describe the rough sea surface as a zero-mean Gaussian random process [13]. The surface is described as a linear superposition of sinusoidal ocean waves with a power spectral function that is plotted in Fig. 2 for three different wind speeds. The plots show that higher wind speeds give rise to longer ocean waves, whereas the small scale waves are relatively unaffected by the wind speed and are observed riding on top of the long waves as seen in Fig. 3 (which also includes a target). This is characteristic of a multiscale rough surface.

The ocean waves evolve with time according to a linear gravity/capillary wave dispersion relation as described in [14]–[17]. Fig. 3 shows a ship-like target on a time-evolving sea surface at time zero and after 5 s, with a wind speed of 15 m/s. Note that the vertical scales are somewhat exaggerated in this figure. Also note that the target moves up and down with the long waves, but does not rotate or move side-to-side. The target is joined with the sea surface in such a way that the target height above water is always the same with respect to the point where the left side of the hull meets the water (i.e., the illuminated side). This simple approach insures that the variations observed in the RCS are not

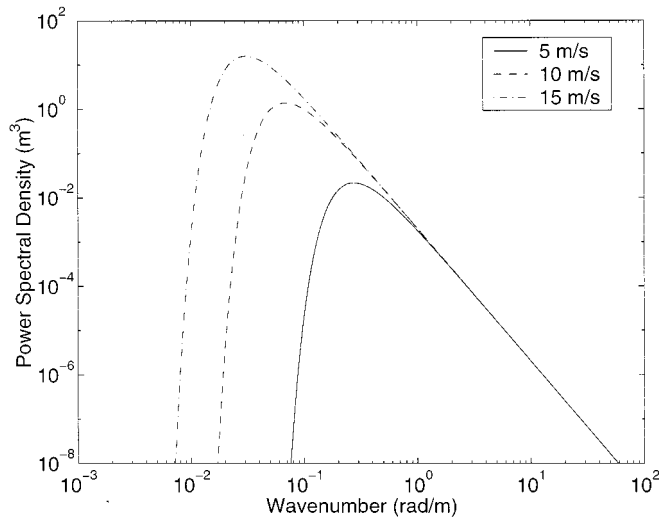


Fig. 2. Pierson–Moskowitz ocean wave spectrum for different wind speeds.

due to a changing target surface area. A more sophisticated hydrodynamics model is needed to analyze the rolling and pitching of the target on the waves, and would require knowledge of the mass distribution of the floating target. This study may be performed in the future.

The scattered fields are found using the method of moments [18] to discretize the electric field integral equation (EFIE) over the composite target and sea surface of Fig. 1 or Fig. 3. The unknown surface currents are expanded with 10 pulse basis functions per wavelength. The SAGFB method is then used to efficiently solve the resulting system of equations [2]. The geometry is illuminated by an incident plane wave of infinite extent, so therefore the endpoints of the finite sea surface model will also contribute to the scattered field. To minimize this unwanted endpoint scattering, tapered resistive cards are placed on the last 10 wavelengths at both ends of the surface using an approach similar to that used in [19]. This model has been validated in [1] and [2] by varying the length of the sea surface, and by comparison with a reference solution of a target on an infinite flat surface as discussed in the next section.

It should be mentioned here that the rough sea surface will also contribute to the computed backscatter (i.e., sea clutter), and is proportional to the length of the surface in the numerical model. However, it has been shown in [1] that the low-angle sea clutter is relatively insignificant compared with the target scattering when using the linear Pierson–Moskowitz ocean model and a finite surface. This model does not produce wave crests, white caps, or breaking waves, which are primarily responsible for sea clutter at low angles of incidence [14], [16]. Some sea clutter results are included in the next section for comparison with the total scattering which is expected to be dominated by the target.

III. NUMERICAL RESULTS

The backscattered field for plane wave incidence is plotted in the form of 2-D radar cross section (2-D RCS), or “radar echo width,” which is defined as

$$2D \text{ RCS} = \lim_{\rho \rightarrow \infty} 2\pi\rho \frac{|E^s(\bar{\rho})|^2}{|E^i|^2} \quad (1)$$

where $\bar{\rho}$ is the vector from the target to the receiver, and $|E^i|$ and $|E^s(\bar{\rho})|$ are the magnitudes of the incident and scattered electric fields. The plot units are in decibels relative to a meter (dBm). The electric field is horizontally polarized and the frequency is 1 GHz throughout the following. The wavelength λ is 0.3 m.

The two target geometries shown in Fig. 4 are used for this analysis. The target of Fig. 4(a) is a ship-like target with a vertical hull. This corresponds to an end-on view of a three-dimensional (3-D) ship which is illuminated broadside in azimuth. The hull forms a 90° corner reflector with a flat sea surface, so the RCS is expected to be very high for calm seas. The deck house on top of the ship also forms a smaller 90° corner reflector. The target of Fig. 4(b) is a low-observable shape which is expected to have a low RCS when the elevation angle of the incident plane wave is close to grazing the sea surface. It will have a higher RCS as the elevation angle approaches 20° , where the plane wave is normally incident on the sloped side. At the frequency of 1 GHz the ship-like target is 43.33λ high and the low-RCS target is 30λ high.

The range of validity of the finite sea surface model has been demonstrated in [1] and [2] by comparison with a target on an infinite flat surface. The infinite surface result is computed using the MoM with a ground plane Green’s function. The target is placed near the right end of each finite surface and the plane wave is incident from the left, so a very large portion of the surface in front of the target is illuminated. The finite surface results have an error of less than about 0.5 dB compared with the infinite surface results for all elevation angles above a certain grazing angle threshold determined by the height of the target and the length of the surface. For the targets of interest here, this threshold is calculated approximately as 2° for a 400 m surface and 0.4° for a 1200 m surface, and is supported by comparison with the infinite flat surface result.

To demonstrate the effect of the surface roughness, Fig. 5 shows the backscatter versus elevation angle patterns of the targets on a set of stationary rough surfaces with different wind speeds. Each surface is 400 m long and is a single randomly generated realization of a Pierson–Moskowitz ocean surface for the given wind speed. The RMS surface roughness for each case is as follows: 0.135 m for the 5 m/s wind speed, 0.54 m for 10 m/s wind speed, and 1.22 m for the 15 m/s wind speed. The finite flat surface result is also plotted. It is seen that higher wind speeds tend to lower the RCS of the ship-like target because the strong 90° corner reflector formed by the surface and the ship’s hull is broken up by the rough surface. It is also observed that the 5 m/s and 10 m/s patterns tend to converge to the flat surface case for low elevation angles (keeping in mind that these results are valid down to 2° grazing). This is consistent with rough surface scattering theory because it is expected that the specular scattering of the incident plane wave from the surface becomes more coherent for low angles [3] [20]. The scattering patterns for the low-RCS target are about 40 dB below the ship-like target, except when the elevation angle approaches 20° which is broadside to the sloped side. There appears to be a strong interference between two comparable scattering features, probably due to the direct and sea-reflected scattering from the sloped side. A more complete Monte Carlo study of the angular scattering from these targets is presented in [3].

The total sea clutter for the 15 m/s wind speed is also plotted in Fig. 5(b), i.e., the scattering from the 400 m surface with the target absent. (Note that the total sea clutter is in the same units as 2-D RCS and is not normalized to surface length. As noted in the previous section, the total sea clutter is expected to grow proportionally to the length of the surface included in the numerical model.) The clutter is about 10–20 dB lower than the total scattering for the low-RCS target, and 40–50 dB lower than the total scattering for the ship-like target, so it is safe to assume that the scattering is dominated by the targets for these cases. The envelope of the sea clutter decreases with angle, as expected for the linear ocean model used here.

The backscatter as a function of time for the two targets on a 400 m time-evolving rough surface is plotted in Fig. 6 for different wind speeds. The elevation angle of the incident plane wave is 5° . At time zero the surfaces are the same as used in Fig. 5 and evolve with time ac-

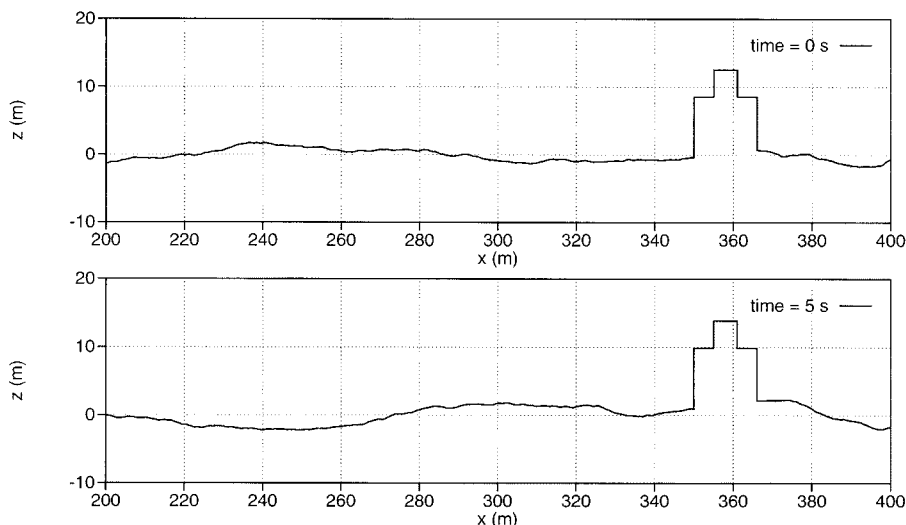


Fig. 3. The 13 m ship-like target on a time-evolving sea surface at time zero and after 5 s. Wind speed = 15 m/s.

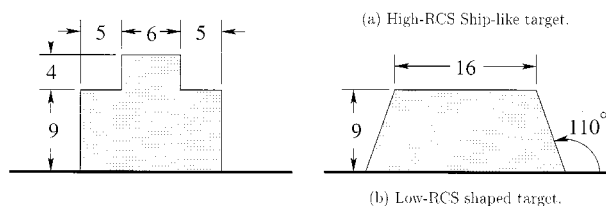


Fig. 4. Two target geometries considered in the analysis. Dimensions are in meters.

ording to the linear dispersion relation. The total sea clutter as a function of time is also plotted for the 15 m/s wind speed case in Fig. 6(b). The ship-like target shows very small variations for the 5 m/s wind speed, but large variations for the 15 m/s wind speed. Furthermore, the RCS is always less than the flat surface case as was also true in Fig. 5(a). On the other hand, the low-RCS target shows large variations for both wind speeds, and the RCS is frequently higher than the flat surface case. This is probably due to the rapidly varying interference pattern observed in Fig. 5(b) near 5° elevation, which also has about the same range of variation in the RCS. If the elevation angle had been chosen to correspond to a local maxima in the flat surface RCS versus angle pattern, then the RCS versus time plots for the rough surfaces are expected to be lower than the flat surface case.

Fig. 7 shows backscatter versus time for the two targets on a 1200 m time-evolving rough surface. The elevation angle in this case is 0.4°, which is a realistic low-grazing angle for surface search radars. The total sea clutter for this case is below -30 dB so it does not show up on the plot. The incident field is expected to be highly coherent for this case, and as the figure shows, the variations in the RCS are considerably less than for the 5° elevation angle of Fig. 6.

It is also interesting to observe that the 15 m/s wind speed results seem to exhibit a wave-like pattern similar to the Pierson–Moskowitz ocean surface model. In a preliminary attempt to correlate this with the geometric variations in the sea surface, Fig. 8 plots the vertical displacement of the ship-like target as it moves up and down on the waves. The elevation of the point where the left side of the target meets the sea surface is plotted. (Recall from Section II that the same portion of the target remains above water.) It is seen that the slow variation in the RCS versus time plot of Fig. 7(a) roughly follows the movement of the target. The maximum RCS occurs when the ship is on a crest and the minimum occurs when the ship is in a trough. This suggests that the

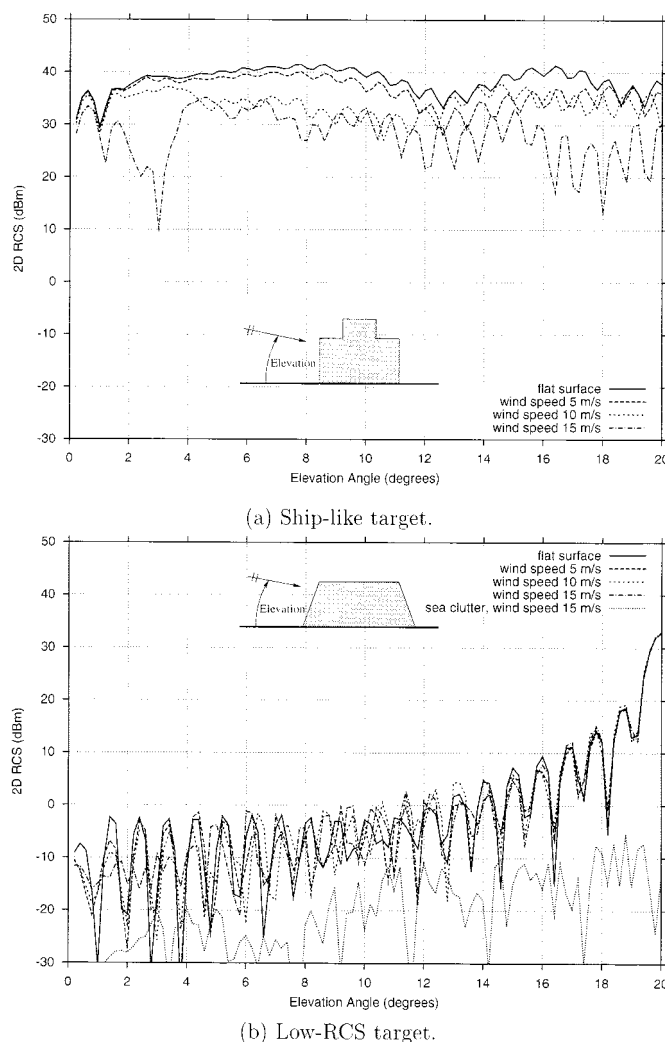
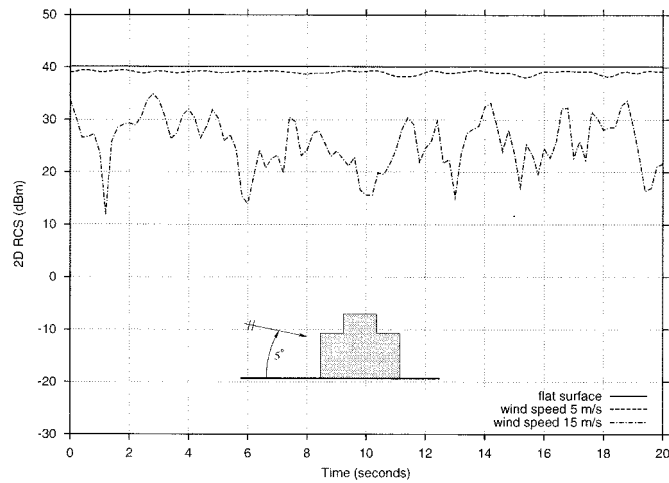
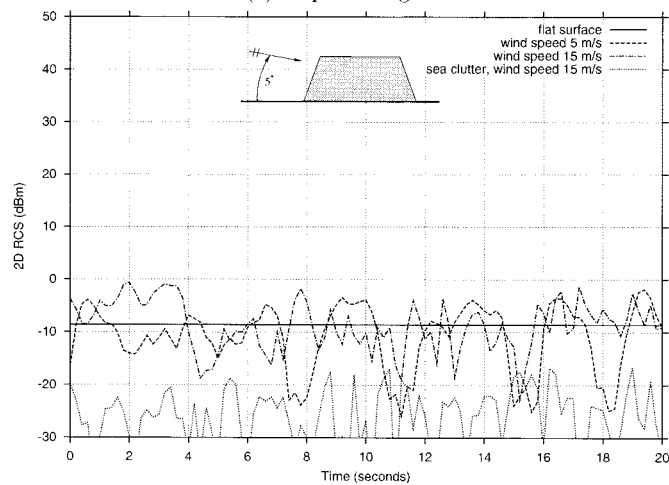


Fig. 5. Backscatter versus elevation angle for two targets on a rough sea surface for different wind speeds. Surface is 402.4 m long, horizontal polarization, frequency = 1 GHz.

sea surface influence on the RCS of targets for low-grazing angles depends mainly on the long waves in the vicinity of the target. The slope



(a) Ship-like target.



(b) Low-RCS target.

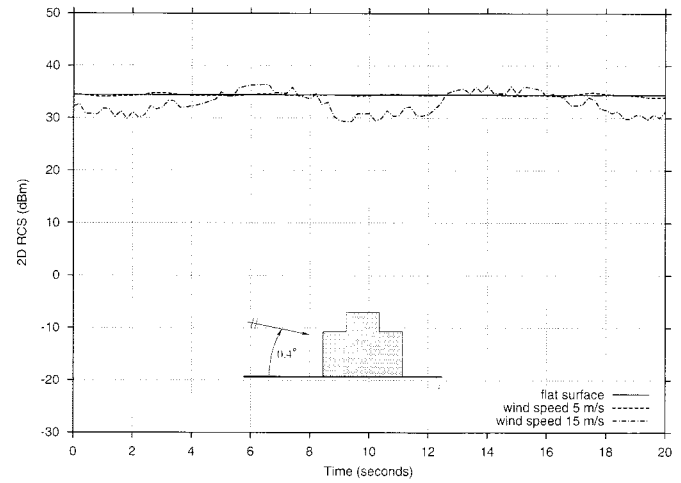
Fig. 6. Backscatter versus time for two targets on a time-evolving sea surface for different wind speeds. Surface is 402.4 m long, horizontal polarization, frequency = 1 GHz, elevation angle = 5° .

of the long waves in the vicinity of the target may also be a factor, especially for the ship-like target because a nonzero slope breaks up the 90° corner reflector effect.

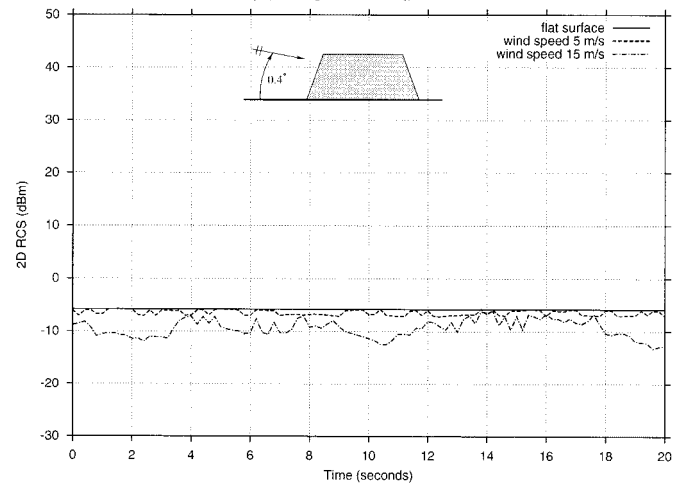
To investigate this further, Fig. 9 plots the magnitude of the *modulation transfer function* (MTF) which correlates the backscatter to the horizontal component of the long surface wave orbital velocity [21]. It is noted that the MTF is roughly calculated for this single time-evolving surface realization without using ensemble averages. The wind speed is 15 m/s and the horizontal component of the orbital velocity is calculated at the point where the left side of the target meets the sea surface. The MTF is plotted in the frequency domain. It is seen that the backscatter is highly correlated with the long wave frequency of about 0.12 Hz for the ship-like target for the low grazing case (0.4° elevation), as suggested from the corresponding RCS result of Fig. 7(a). The other cases are only moderately correlated with the long waves. A more detailed study of the correlation between long ocean waves and ship RCS is warranted for future work, perhaps using a Monte Carlo approach; such an investigation is beyond the scope of this communication.

IV. CONCLUSION

The results of this communication have shown that the rough sea surface influence on the RCS of 2-D targets depends on many factors.



(a) Ship-like target.



(b) Low-RCS target.

Fig. 7. Low-grazing angle backscatter versus time for two targets on a time-evolving sea surface for different wind speeds. Surface is 1200 m long, horizontal polarization, frequency = 1 GHz, elevation angle = 0.4° .

In general, the variation in the RCS is larger for higher wind speeds and higher elevation angles. This is expected from a consideration of the incident field in the presence of the rough surface, which becomes more coherent for low elevation angles. The target geometry also determines how the rough sea can influence the RCS. It is observed that the rough surface tends to reduce the RCS of the ship-like target compared with the flat surface case, both as a function of elevation angle and time, because the 90° corner reflector formed by the vertical hull and the sea surface is broken up when the surface becomes rougher. The RCS of the low-RCS target on a rough surface may vary above and below the flat surface case.

The low-grazing angle RCS versus time results show relatively small variations in the RCS, as one might expect because the incident field is highly coherent. However, there is also observed a wave-like dependence which correlates with the vertical movement of the target floating on the waves. This suggests that the long waves in the ocean spectrum are primarily responsible for the variations in the RCS for low-grazing angles, possibly due to the reduced visibility of the target when it is in a trough, and/or the slope of the long waves in the vicinity of the target. A more thorough statistical investigation is warranted for future work.

The variations in the RCS as a function of time happen over a time scale of seconds, which is much longer than the pulse width and pulse

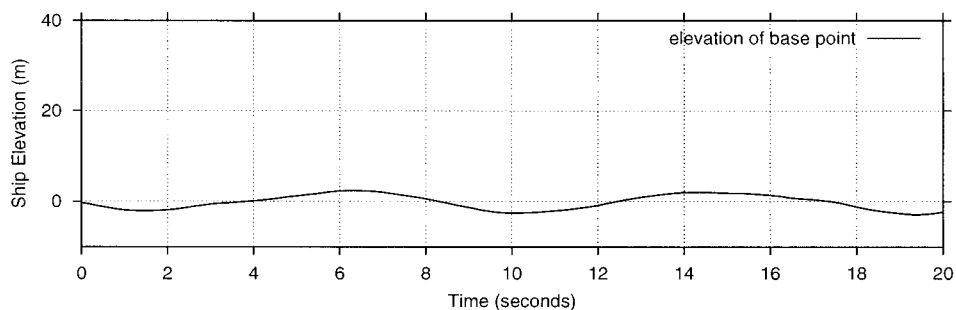


Fig. 8. Plot of the vertical displacement of the base of the target as it moves up and down on the waves. Wind speed = 15 m/s.

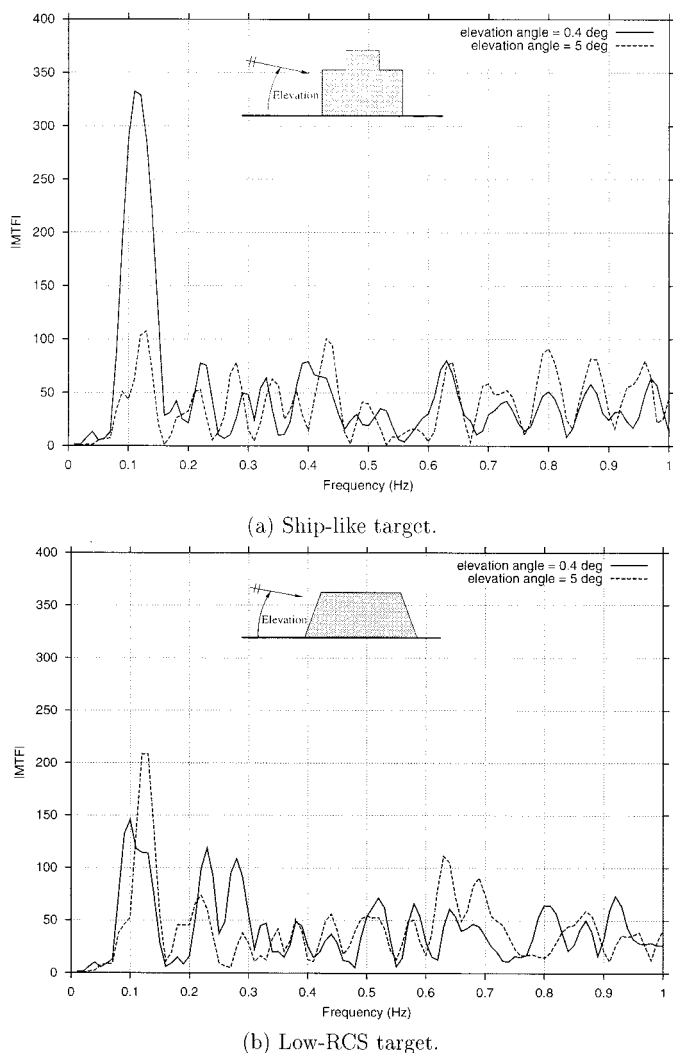


Fig. 9. Magnitude of modulation transfer function (MTF). Surface is 1200 m long for 0.4° case and 400 m long for 5° case. Wind speed = 15 m/s, horizontal polarization, frequency = 1 GHz.

repetition rate of most radars. Furthermore, this slow variation is unlikely to have much effect on the Doppler spectrum. This is why it is important to begin to understand the time-changing nature of the scattering from a target on the sea. Future studies could extend the results to vertical polarization, higher frequency bands, and three dimensional problems. (Some initial results for 3-D are reported in [22].) It would also be of interest to include the rolling and pitching of a floating target via a proper hydrodynamics model, and to compare the numerical re-

sults with experimental data should such data become available in the future.

ACKNOWLEDGMENT

The authors would like to thank B. Ungan and Dr. J. T. Johnson, Department of Electrical Engineering, The Ohio State University, for providing computer subroutines for generating the time-evolving Pierson–Moskowitz sea surface, and their technical assistance.

REFERENCES

- [1] M. R. Pino, L. Landesa, J. L. Rodríguez, F. Obelleiro, and R. J. Burkholder, "The generalized forward-backward method for analyzing the scattering from targets on ocean-like rough surfaces," *IEEE Trans. Antennas Propagat.*, vol. 47, pp. 961–969, June 1999.
- [2] M. R. Pino, R. J. Burkholder, and F. Obelleiro, "Spectral acceleration of the generalized forward-backward method," *IEEE Trans. Antennas Propagat.*, to be published.
- [3] R. J. Burkholder, M. R. Pino, and F. Obelleiro, "A Monte Carlo study of the rough sea surface influence on the radar scattering from 2-D ships," *IEEE Antennas Propagat. Mag.*, vol. 43, pp. 26–33, Apr. 2001.
- [4] J. T. Johnson and R. J. Burkholder, "Coupled canonical grid/discrete dipole approach for computing scattering from objects above or below a rough interface," *IEEE Trans. Geosci. Remote Sensing*, vol. 39, pp. 1214–1220, June 2001.
- [5] T. Chiu and K. Sarabandi, "Electromagnetic scattering interaction between a dielectric cylinder and a slightly rough surface," *IEEE Trans. Antennas Propagat.*, vol. 47, pp. 902–913, May 1999.
- [6] E. A. Shtager, "An estimation of sea surface influence on radar reflectivity of ships," *IEEE Trans. Antennas Propagat.*, vol. 47, pp. 1623–1627, Oct. 1999.
- [7] —, "A study of the four-path model for scattering from an object above a halfspace," *Microwave Opt. Tech. Lett.*, vol. 30, no. 2, pp. 130–134, July 2001.
- [8] J. T. Johnson, "A numerical study of scattering from an object above a rough surface," *IEEE Trans. Antennas Propagat.*, to be published.
- [9] H.-T. Chou and J. T. Johnson, "A novel acceleration algorithm for the computation of scattering from rough surfaces with the forward-backward method," *Radio Sci.*, vol. 33, pp. 1277–1287, Sept./Oct. 1998.
- [10] D. Holliday, L. L. DeRaad, and G. J. St-Cyr, "Forward-backward: A new method for computing low-grazing angle scattering," *IEEE Trans. Antennas Propagat.*, vol. 44, pp. 722–729, 1996.
- [11] D. A. Kapp and G. S. Brown, "A new numerical method for rough surface scattering calculations," *IEEE Trans. Antennas Propagat.*, vol. 44, pp. 711–721, May 1996.
- [12] G. S. Brown, "Special issue on low-grazing-angle backscattering from rough surfaces," *IEEE Trans. Antennas Propagat.*, vol. 46, pp. 1–2, Jan. 1998.
- [13] W. J. Pierson and L. Moskowitz, "A proposed spectral form for fully developed wind seas based on the similarity theory of S. A. Kitaigorodskii," *J. Geophys. Res.*, vol. 69, pp. 5181–5190, 1964.
- [14] C. L. Rino, T. L. Crystal, A. K. Koide, H. D. Ngo, and H. Guthart, "Numerical simulation of backscatter from linear and nonlinear ocean surface realizations," *Radio Sci.*, vol. 26, no. 1, pp. 51–71, Jan.–Feb. 1991.
- [15] B. Ungan and J. T. Johnson, "Time statistics of propagation over the ocean surface: A numerical study," *IEEE Trans. Geosci. Remote Sensing*, vol. 38, pp. 1626–1634, July 2000.